

## Supplementary Information

### **A peptide inhibitor of the complex AIF/CypA is neuroprotective against oxidative stress**

Nunzianna Doti <sup>(1,2,3)\*</sup>, Christina Reuther <sup>(2)</sup>, Pasqualina Liana Scognamiglio <sup>(1)</sup>, Amalia Mihaela Dolga <sup>(2)</sup>, Nikolaus Plesnila <sup>(3,4)\*</sup>, Menotti Ruvo <sup>(1)</sup>, Carsten Culmsee <sup>(2)\*</sup>.

<sup>(1)</sup>Institute of Biostructures and Bioimaging (IBB)-CNR, CIRPEB; Via Mezzocannone, 16, 80134, Napoli, Italy; <sup>(2)</sup>Institute of Pharmacology and Clinical Pharmacy, Philipps University of Marburg, 35032, Marburg, Germany; <sup>(3)</sup>Department of Neurodegeneration, Royal College of Surgeons in Ireland, Dublin 2, Ireland; <sup>(4)</sup>Institute for Stroke and Dementia Research (ISD) Großhadern Max-Lebsche Platz 30, D-81377, Munich, Germany.

\*Corresponding authors: Dr. Nunzianna Doti, Institute of Biostructures and Bioimaging (IBB)-CNR, and CIRPEB; Via Mezzocannone, 16, 80134, Naples, Italy; Phone: +39 081 2536644, Fax: +39 081 2534574; E-Mail: nunzianna.doti@cnr.it; Prof. Dr. Carsten Culmsee, Institute of Pharmacology and Clinical Pharmacy, Philipps University of Marburg, 35032, Marburg, Germany; Karl-von-Frisch-Straße 1, 35032 Marburg, Phone: +49-(0)6421 – 2825963, Fax: +49-(0)6421 – 2825720, E-Mail: culmsee@staff.uni-marburg.de Prof. Dr. med. Nikolaus Plesnila, Institute for Stroke and Dementia Research (ISD), University of Munich Medical School – Campus Großhadern Max-Lebsche Platz 30; 81377 Munich, Germany, Phone: +49 (0)89 7095 – 8357, Fax: +49 (0)89 7095 – 8369, E-Mail: nikolaus.plesnila@med.uni-muenchen.de.

## Supplementary Legends

**Supplementary Figure 1: Bio-physical characterization of tAIF and CypA.** (A) SDS-PAGE of tAIF (~ 57KDa) and CypA (~ 18 KDa) after purification steps. tAIF and CypA were efficiently produced in a soluble form when recombinantly overexpressed in *E. coli* and could be purified to almost homogeneity (Supplementary Materials and Methods). (B) CD spectra of AIF (blue) and CypA (green) in phosphate buffer 10 mM pH 7.4. The concentration of proteins were 5  $\mu$ M and 10  $\mu$ M for tAIF and CypA, respectively. Both proteins appeared correctly folded in aqueous buffer. (C) Aminoacidic sequence and molecular weight (MW) of AIF peptides. (D, E) Structural characterization of AIF peptides. AIF peptides were structurally characterized by CD spectroscopy. In aqueous buffer, both peptides gave a complex spectrum with a large negative band at around 198 nm and a shoulder in the 220–230 nm range, indicating the occurrence of mixed random coil and other poorly defined structures. To probe their potential conformational preferences, we used TFE, which is known to stabilize the folding of peptides prone to adopt  $\alpha$ -helical structures. Addition of TFE to AIF(343-360) induced a canonical  $\alpha$ -helix folding (C), witnessed by a maximum at 192 nm and two minima at 208 and 222 nm. Addition of increasing amounts of TFE to AIF(370-394) instead, induced only a limited conversion toward an  $\alpha$ -helix structure. Indeed, the difference spectrum between spectra with 50% TFE and 0% TFE, shown in D (dotted line), is consistent with a very small amount of  $\alpha$ -helical content with a maximum at 192 nm and two minima at 208 and 222 nm, in agreement with the crystallographic structure showing that in this region the protein adopts a  $\beta$ -strand conformation. (F) Detection of PPIase activity. The activity of CypA was determined by measuring the catalysis of the cis  $\rightarrow$  trans interconversion (■) in the absence of CypA; (▲) in the presence of 0.2  $\mu$ M of CypA and 20  $\mu$ M of Chymotrypsin; (▼, ▲, ●) in the presence of 0.2  $\mu$ M of CypA and 20  $\mu$ M of Chymotrypsin and 0.2, 2, 20  $\mu$ M of AIF(370-394), respectively; (□, ◆) in the presence of 0.2  $\mu$ M of CypA and 20  $\mu$ M of Chymotrypsin and 0.2 and 1  $\mu$ M of CsA, respectively. No inhibition of catalytic activity of CypA were observed by AIF(370-394) peptide compared to CsA.

**Supplementary Figure 2: Glutamate-induced subcellular trafficking of AIF and CypA.** (A) Time-course of AIF cellular localization upon glutamate insult were detected by western blot. AIF appeared in the nucleus at about 10-12 h upon glutamate treatment. (B, C) Immunofluorescent staining of AIF and CypA detected in HT-22 treated with 2 mM glutamate and untreated (Ctrl) for the indicated times. Representative cells are shown. Bar: 10  $\mu$ m. (D) Co-immunoprecipitation of AIF and CypA in glutamate-treated (2 mM for 12-14h) and untreated cells. After immunoprecipitation of CypA and immunodetection of AIF or CypA, we found that AIF was

captured only in apoptotic cells (upper panel). The panel on the right shows a Western blot analysis of the total amount of AIF and CypA, using as loading marker the Tubulin protein

**Supplementary Figure 3: The down-regulation of H2AX doesn't provides protective effects upon glutamate treatment.** (A) HT-22 cells were transfected with scrambled siRNA (siCtrl) or with siRNA against mouse H2AX (siH2AX). Total cell lysates from siRNA-treated cells were prepared and the mRNA levels of H2AX were assessed by RT-PCR. (B) Cell viability after downregulation of H2AX were assessed by MTT assay. The wild type and H2AX knockdown HT-22 cells were treated or untreated (control) with 2 mM glutamate for 12h. MTT results are presented as percentage of control, considered to be 100%, and represent mean  $\pm$  SD of three independent experiments. (C) Cell mortality in H2AX-downregulated HT-22 cells upon glutamate treatment (2 mM at 0h; n = 8) was also assessed over a time period of about 15h by impedance measurement. Data show that the depletion of H2AX doesn't prevent glutamate-mediated apoptosis in HT-22 cell lines.

**Supplementary Figure 4: Evaluation of cellular uptake of peptides in HT-22 neuronal cells.** (A) Evaluation of possible cytotoxic effects of vehicle (Pro-Ject™ Protein Transfection Reagent kit, PIERCE) used to transfect peptides in HT-22 cells. Differences in cell viability were evaluated by MTT assays in cells treated and untreated with glutamate. Results show that the vehicle was inert toward cells under both conditions. Results are presented as percentage of controls considered to be 100% and represent the means  $\pm$  SD of at least four independent experiments performed in quadruplicate. (B) Fluorescent microscopy analysis of intracellular distribution of FITC (fluorescein isothiocyanate)-conjugated synthetic peptides. Images obtained showed that FITC-conjugated peptides were efficiently transfected in HT-22 cells. Bar: 10  $\mu$ m. (C) Quantification of cells transfected with FITC-conjugated peptides by Flow-cytometry analysis. An high percentage of cells appeared to be transfected.

**Supplementary Figure 5: CypA downregulation provided protective effect at level of mitochondria.** (A) After 12 h post-glutamate treatment, wild type and CypA-downregulated HT-22 cells were labeled with TMRE, and the frequency of cells with  $\Delta\Psi$ m loss was assessed by FACS analysis. Data show that the silencing of CypA before the glutamate insult, was sufficient to prevent loss of red fluorescence thus suggesting that essential mitochondrial functions are restored. Data

presented in the bar chart are means of three independent experiments  $\pm$  SD and are expressed as percentage of control considered as 100%. **(B)** Quantification of mitochondrial morphology of ~500 cells per condition: category 1 (elongated tubulin-like structure), category 2 (intermediate length) and category 3 (fragmented mitochondria).  $**p < 0.01$  compared with glutamate 2 mM-treated cells (n = 3 independent experiments, ANOVA, Bonferroni-test).

**Supplementary Figure 6: The silencing of CypA restored intracellular  $\text{Ca}^{2+}$  concentration in HT-22 cells treated with glutamate.** **(A)** Dose-dependent increase of intracellular  $\text{Ca}^{2+}$  divalent ion concentration induced by glutamate treatment for 12 h, as detected by the fluorescent  $\text{Ca}^{2+}$  indicator Fluo4. Data are the means  $\pm$  SD (n = 8). **(B)** Downregulation of CypA restored intracellular  $\text{Ca}^{2+}$  concentration at level comparable to those of untreated cells (Veh). Data are the means  $\pm$  SD (n = 8).  $**p < 0.01$  compared with glutamate 2 mM-treated cells (n = 3 independent experiments, ANOVA, Bonferroni-test).

## Supplementary Materials and Methods

**Plasmid preparation, expression and purification of AIF(1-121).** Mouse AIF deletion mutant (AIF $\Delta$ 1-121, named tAIF) and mouse CypA was amplified by PCR from the pcDNA3.1-AIF and pcDNA3.1-CypA full length plasmids, which were used as template in a reaction mixture with the Fusion polymerase (Finnzymes, F-530L, 500 U, New England BioLabs). The PCR products were cloned in the pETM11 for AIF and pETM13 for CypA (EMBL, Germany) vector caring NcoI-XhoI restriction sites, followed by sequencing (Sigma-Aldrich, Italy). tAIF deletion mutant and full length CypA were expressed as His<sub>6</sub>-tagged proteins in *E.coli* BL21(DE3) with 1 mM isopropyl 1-thio- $\beta$ -D-galactopyranoside (IPTG). His<sub>6</sub> fusion proteins were recovered on a 5 mL His-Trap columns (GE Healthcare Europe GmbH, Milano, Italy). Following affinity purification, the His<sub>6</sub> tags of the recombinant fusion proteins were cleaved off by digestion with the TEV and Thrombin (Sigma-Aldrich 27-0846-01, Italy) proteases for tAIF and CypA, respectively. Pure recombinant proteins were recovered after another step of purification on a 1 mL His-Trap column (GE Healthcare Europe GmbH, Milano, Italy). Purity was assessed by SDS/PAGE.

**CD analysis.** Far-UV wavelength CD spectra of proteins and peptides were recorded from 260 to 190 nm on Jasco J-720 spectropolarimeter (Jasco, Tokyo, Japan). The parameters used were as follows: bandwidth, 1 nm; step resolution, 0.25 nm; scan speed, 50 nm/min; response time, 0.2 s. Each spectrum was obtained after an average of four scans. The protein concentrations were 5  $\mu$ M and 10  $\mu$ M for tAIF and CypA, respectively. The peptide concentration was typically 80  $\mu$ M in sodium phosphate buffer, pH 7.4; various ratios of TFE/water mixture. CD intensity is expressed in terms of mean molar ellipticity ( $[\theta]$ , expressed in deg cm<sup>2</sup> dmol<sup>-1</sup>) according to the following equation:  $[\theta_m] = \theta_{mdeg} / lCN$ , where  $\theta_{mdeg}$  is the measured ellipticity in millidegrees,  $l$  is the cell path length in cm;  $C$  is the molar concentration of the protein or peptide;  $N$  is the number of residues in the peptide or protein.

**AIF and CypA immunofluorescent assessment.** HT-22 were fixed in 4% PFA, permeabilized with 0.04 % Tween 20, incubated with an anti-AIF (Santa Cruz, #sc-9416) or anti-CypA (Cell Signaling, #2175) antibodies, and detected by an anti-mouse IgG conjugated with Alexa<sup>®</sup> Fluor 568. Cells were counterstained with the DNA-binding dye 4',6-diamidino-2-phenylindole dihydrochloride (DAPI) (Sigma-Aldrich, Taufkirchen, Germany). Images were acquired using a confocal laser-scanning microscope (Axiovert 200, Carl Zeiss, Jena, Germany). Light was collected through a 63 x 1.4 NA oil immersion objective.

**Cell viability.** Quantification of cell viability of HT-22 cells incubated with Pro-Ject<sup>™</sup> Protein Transfection Reagent kit according to the manufacturer's instructions (Pierce Prod # 89850) was performed by MTT reduction assay. The absorbance of each well was determined with an

automated FLUOstar Optima reader (BMG Labtechnologies GmbH, Inc. Offenburg, Germany) at 570 nm with a reference filter at 630 nm. The control cell values were set to 100% cell viability, since absolute values may vary between experiments. For statistical analysis, the experiments were repeated at least three times with an  $n = 8$  per condition.

**Peptide cellular uptake evaluation.** The cellular uptake assessment of FITC-conjugated peptides were performed by EPI-fluorescence and FACS. HT-22 cells were transfected with FITC-conjugated AIF peptides at concentrations of 50  $\mu\text{M}$  and then fixed in 4% PFA. Images were acquired using a confocal laser-scanning microscope (Axiovert 200, Carl Zeiss, Jena, Germany). Light was collected through a 20 x objective. Peptide fluorescence was also detected using a FACScan (BD Bioscience). At least 10000 events were counted for each sample. Measurements were performed in triplicates and are representative of at least three independent experiments.

**Mitochondrial membrane potential measurements by Flow Cytometry.** Mitochondrial membrane potential of HT-22 cells transfected with a specific siRNA against CypA (siCypA) or unrelated siRNA used as negative control (siCtrl) and then untreated or treated with glutamate 2 mM for 12 h was determined by JC-1 or TMRE reduction according to the manufacture's protocol (Mitoprobe, Invitrogen) and analyzed by subsequent flow cytometry (FACScan, BD Bioscience). Additional controls were treated with CCCP (50  $\mu\text{M}$ ) 5 min before staining to induce mitochondrial membrane depolarization.

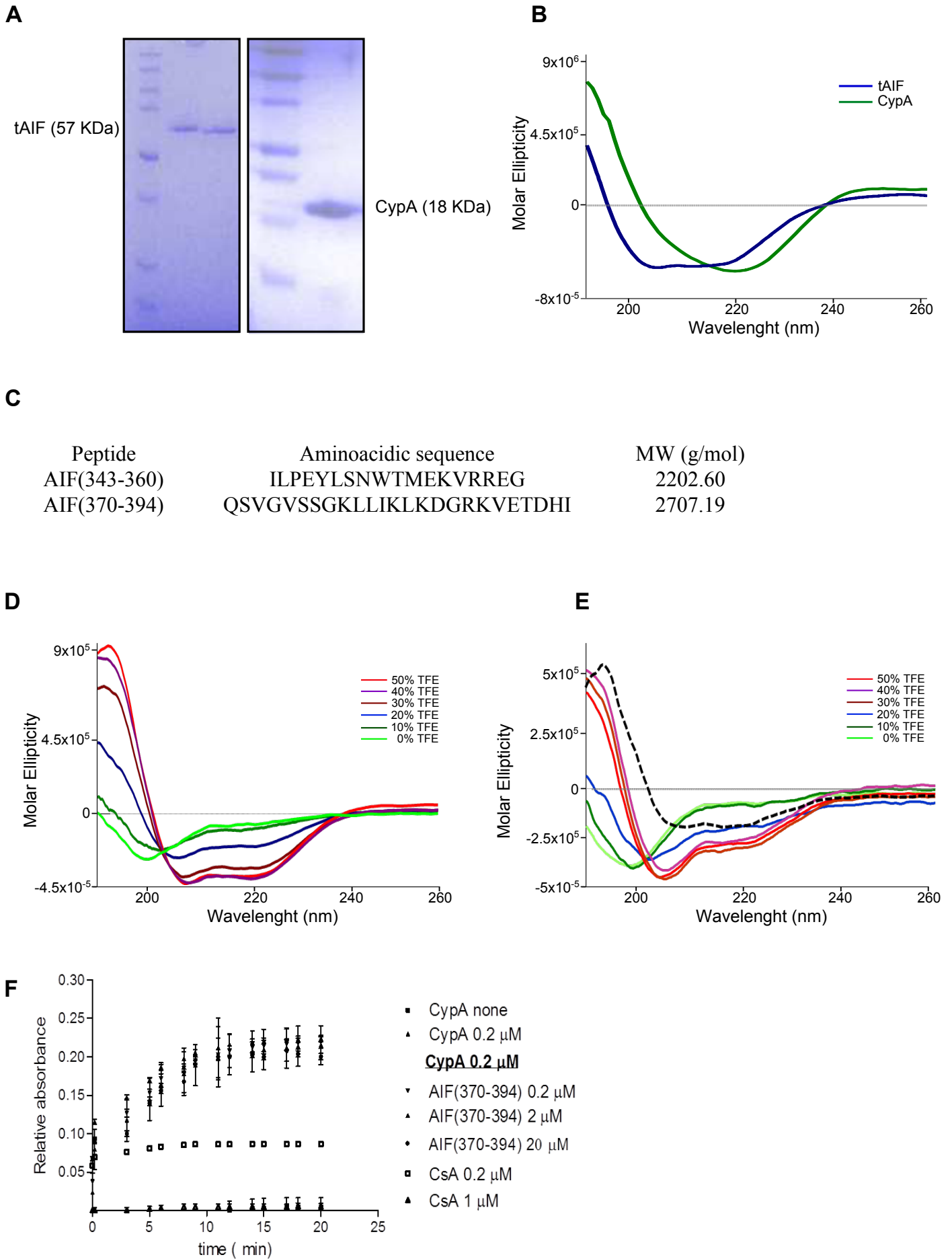
**Evaluation of mitochondrial morphology.** HT-22 cells were labeled with MitoTracker DeepRed according to the manufacturer's protocol (Invitrogen, Germany). Cells were treated with glutamate (2 mM) in the presence or absence of siRNAs for 12-14 h, followed by fixation with 4% PFA and DAPI counterstained for the nuclei. We distinguished three categories of mitochondria based on their morphology: category I, long, tubular mitochondria; category II, short tubules or large round organelles; category III, small fragmented mitochondria. Images were collected with a DMI6000B fluorescence microscope, equipped with a DCF360FX-camera (Leica, Wetzlar, Germany). For statistical analysis, the experiments were repeated at least three times.

**Intracellular  $\text{Ca}^{2+}$  concentration detection.** Intracellular  $\text{Ca}^{2+}$  concentration were assessed using Fluo-4 AM in 96 well plates according to the manufacturer's protocol (Invitrogen). HT-22 transiently transfected with peptides were coated in 96 well plates. After 24 h cells were treated with glutamate 2 mM for 12 h. Intracellular  $\text{Ca}^{2+}$  was detected adding to the medium Fluo-4 AM at 5  $\mu\text{M}$  for 30 minutes. After the washing step, the fluorescence of each well was determined with an automated FLUOstar Optima reader (BMG Labtechnologies GmbH, Inc. Offenburg, Germany) using as excitation wavelength at 485 nm and emission at 520 nm.

**Prolyl isomerase activity assay:** The PPIase activity of CypA was measured as measuring the catalysis of the *cis* → *trans* interconversion of *cis* Suc-Ala-Ala-Pro-Phe-4-pNA substrate (Sigma # S7388) in a coupled assay with α-chymotrypsin (Fischer G 1989 or Zhang X C FEBS Letters 2013). α-Chymotrypsin (21 μM) (Sigma-Aldrich # 6423) was preincubated with the CypA protein (0.2 μM), with two doses (0.2 μM and 2 μM) of AIF(370-394) peptide and then with the substrate (22 μM). Csa at concentration of 0.2 and 2 μM were used as positive control of experiments. Results were performed three times. The hydrolysis of the 4-nitroanilide in the *cis* substrate is limited in rate by the *cis* → *trans* isomerization at Ala-Pro and was followed by the increase in absorbance at 390 nm.<sup>43</sup>

**Statistical analysis.** All data are given as means ± SD. For statistical comparisons between two groups, Student's *t*-test was used assuming a normal distribution of the respective data. Multiple comparisons were performed by ANOVA followed by Scheffé's *post hoc* test. Calculations were made with the Winstat standard statistical software package (Robert Fitch Software, Bad Krozingen, Germany). A statistically significant difference was assumed at \**p* < 0.05, \*\**p* < 0.01, \*\*\**p* < 0.001.

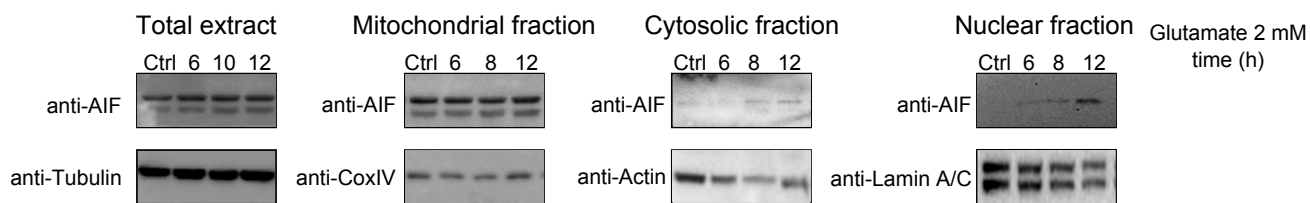
# Supplementary Figure 1



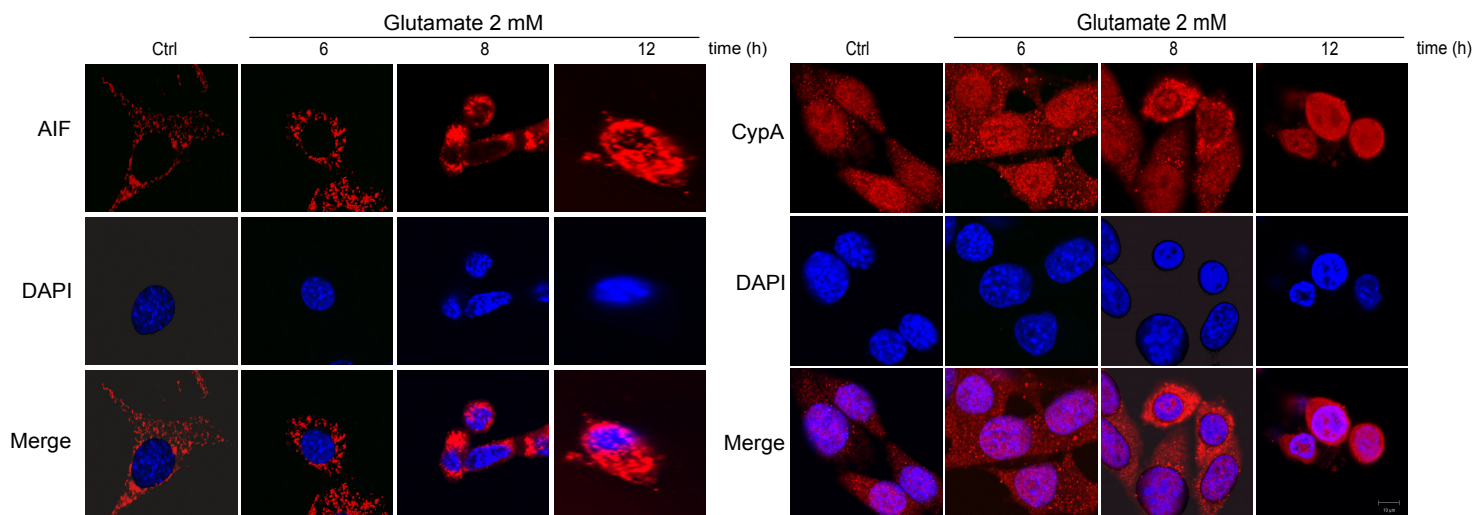


## Supplementary Figure 2

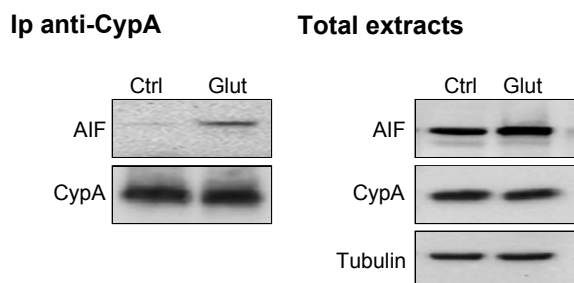
**A**



**B**

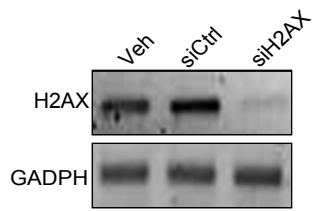


**C**

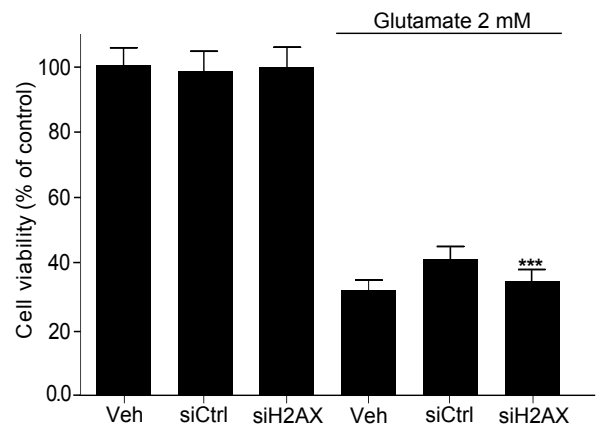


# Supplementary Figure 3

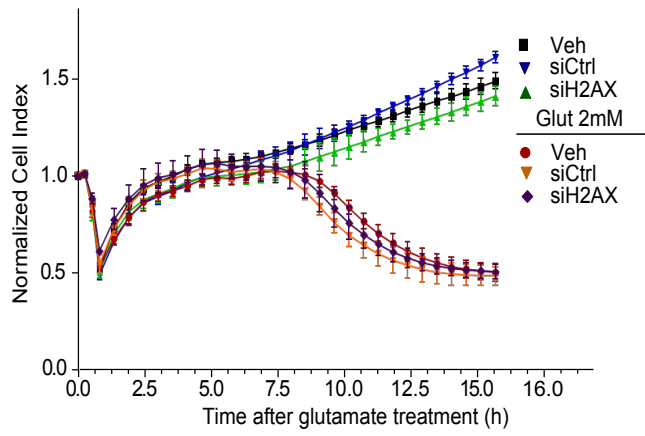
**A**



**B**

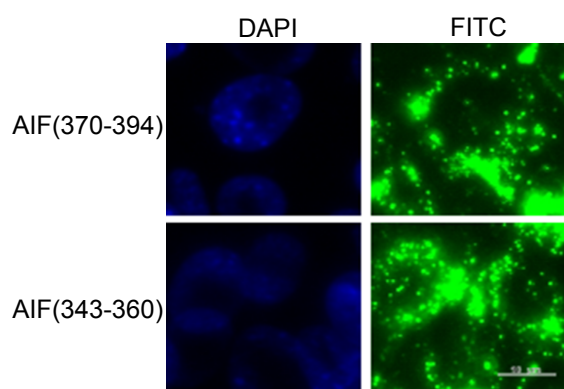


**C**

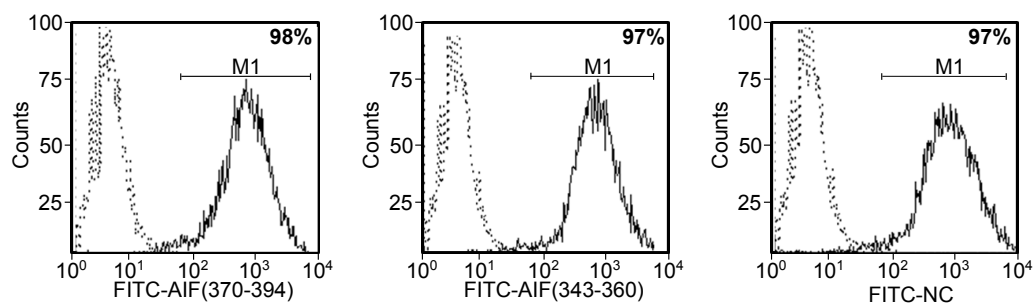


# Supplementary Figure 4

**A**

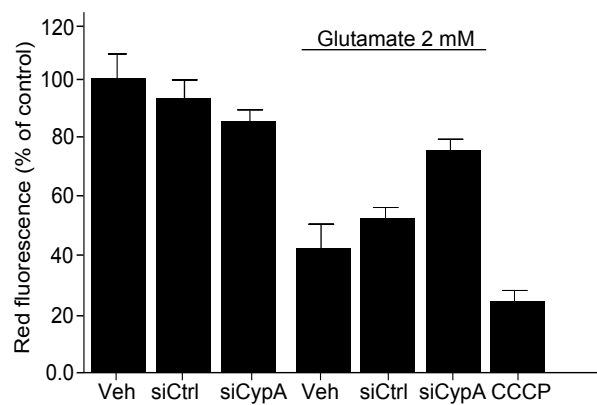


**B**

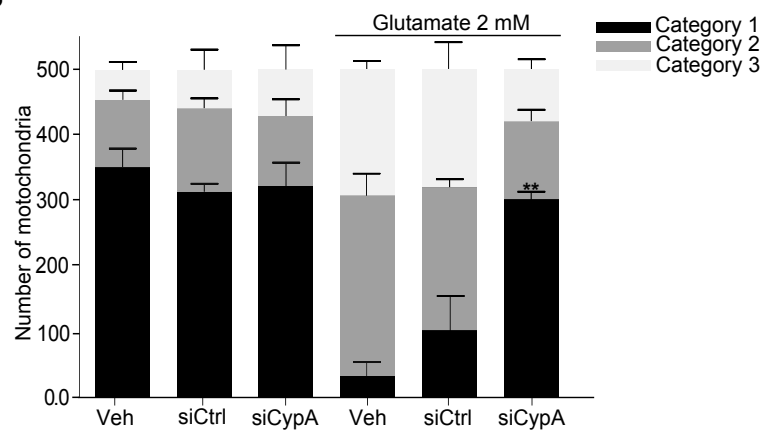


## Supplementary Figure 5

**A**

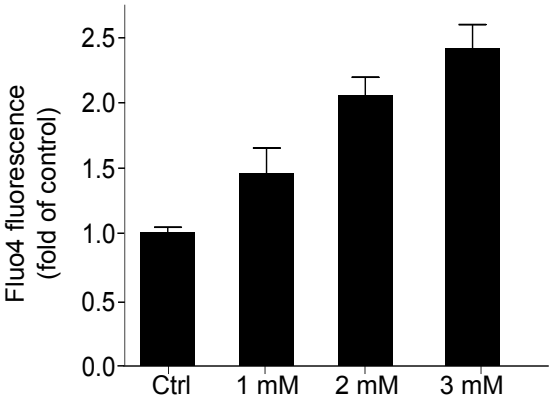


**B**



# Supplementary Figure 6

**A**



**B**

